Springer

KSME

Journal of Mechanical Science and Technology 24 (11) (2010) 2247~2252
www.springerlink.com/content/1738-494x
DOI 10.1007/s12206-010-0811-8

# A mixed analytical-numerical investigation of snap-through of low arches with a power-law variable thickness †

Ali Asghar Atai[1,2,*], Mohammad Hassan Naei[2] and Reza Eghtefari[1]

[1]*Department of Mechanical Engineering, Islamic Azad University, Karaj Branch, Iran*
[2]*Department of Mechanical Engineering University of Tehran, Tehran, Iran*

(Manuscript Received February 1, 2010; Revised June 19, 2010; Accepted July 12, 2010)

**Abstract**

Snap-through is an instability phenomenon that occurs in arch and dome-shaped structures, wherein the structure has to move from a stable equilibrium state through an unstable path into another stable equilibrated configuration in a jumping action. In this study, a linear elastic isotropic low arch is considered as a structure with power-law variable thickness. The phenomenon is investigated by considering the equation of the deflection for the variable thickness arch, solving it with an elegant analytical technique, and finding the snap-through critical load from an extreme condition. The effect of power-law exponent and geometry of the arch centerline on critical load is investigated and the constant thickness case and a very rare case of power-law thickness variation found in literature are considered for verification.

*Keywords*: Snap-through; Low arch; Variable thickness; Power-law; Mixed analytical- numerical

## 1. Introduction

Snap-through is an instability phenomenon that occurs in curved one- and two-dimensional solids, such as shallow arches and shells, that are under the action of a compressive load normal to their continuum. The constraints on these structures are such that external loading causes a compressive internal force to form along or in the plane of the structure. As external loading increases and tries to flatten the structure, this compression builds up and reaches a point that the structure cannot withstand it in a stable equilibrium configuration. Therefore, the structure passes (jumps) through a series of unstable configurations until it reaches another stable equilibrium configuration. This phenomenon has its own applications and adverse effects. It can be used as toggle switches and mechanisms for activating an electrical or mechanical circuit. On the other hand, such jumps can lead to the collapse of a structure and hence to a disaster. Therefore, acquiring suitable knowledge on the phenomenon is of great importance. Several studies and investigations have been carried out on the subject. Timoshenko [1] in 1935 and Biezno [2] in 1938 were among the first who worked on the subject and presented solutions for the cases of distributed and concentrated forces, respectively. Marguerre [3] in 1938 discussed some cases based on the theory of buckling. Fung and Kaplan [4] considered various types of arches and lateral loads. In 1977, Simitses [5] used the energy and deflection methods and considered the variable thickness shallow arches for which the moment of inertia of the cross section varied as the 2nd and ½ power of the horizontal coordinate of the arch. Based on the literature review by the authors, this is the only work that comes close to the present study. Different authors have made attempts to modify or improve the formulation or numerical method for various constant thickness shallow arches with different cross sections, end conditions, or loadings [6-9]. The next section discusses the problem formulation based mainly on the notation used in [5]. The special form of the governing differential equation on the lateral deflection of the arch would allow the use of a very innovative method of analytical solution discussed in Section 3. However, to obtain the critical snap-through loading, it is not possible to continue with the analytical method and a numerical finite difference scheme has to be implemented for this part. Some examples based on the proposed method are discussed in Section 4. Some verifying cases based on previous works as well as the effects of different parameters on critical snap loading are presented.

## 2. Problem formulation

Fig. 1 shows a variable thickness shallow arch. The center-

† This paper was recommended for publication in revised form by Associate Editor Chongdu cho

*Corresponding author. Tel.: +989126016855, Fax: +989126016855
E-mail address: atai@kiau.ac.ir

line equation of the loaded arch is represented by $w$ ($x$) and its undeformed state is denoted by $w_0$ ($x$), in which $x$ shows the horizontal coordinate of the arch. The span of the arch is denoted by $L$ and the maximum height of the centerline is denoted by $e$. For shallow arches, the ratio $e/L$ is considered to be lower than 0.35 [10]. The initial shape of the centerline is considered to be a parabola with the equation

$$w_0(x) = 4ex(L-x)/L^2 . \quad (1)$$

The authors found that for constant thickness shallow arch, the shape of the centerline has very little effect on the critical snap load [11] (in a numerical example, centerlines in the shape of a parabola, as well as circular and elliptical arches, yield the same snap load within less than one percent of difference). The ends are considered to be pinned. This condition causes the development of an axial loading throughout the arch. Moreover, its presence and buildup as the external lateral loading increases are important contributors to the instability of the arch (in an investigation by the authors, when the ends were considered simply supported, i.e., one end pinned and the other roller supported, and hence no axial loading, no snapping occurred and the arch simply went through the initial curved shape to a flat configuration to another curved shape beneath the horizon without any instability and snapping [11]). The thickness is considered to be variable but still small compared to other dimensions of the arch and also symmetrical with respect to $x=L/2$ line. This justifies the decision to consider only the effect of bending moment in formulating the deflection of the arch centerline. This study aims to present the methodology for obtaining critical snap loading. Hence, the loading is considered to be a simple uniformly distributed one with intensity $P$. The deflection of the arch is considered to be small compared to the initial curved shape. Although the structure undergoes considerable displacement by snap through instability, the last assumption is reasonable enough to obtain the critical snap load. Post buckling behavior is not considered here. Fig. 2 shows the free body diagram of a section of the arch in the deformed shape. Based on the moment-curvature relations, the governing equation of the deflection of the arch is

$$w'' - w_0'' + \frac{Qw}{EI(x)} = \frac{Px(L-x)}{2EI(x)} , \quad (2)$$

where $E$ is the modulus of elasticity of the arch material (which is considered to be linear elastic), $I$ ($x$) is the variable area moment of inertia of the arch cross section, and prime denotes differentiation with respect to $x$ coordinate. $Q$ is the unknown axial force resulting in the cross section found by the following procedure. Considering the axial strain of the arch, it can be written (for example see [10]) as

$$\varepsilon = \varepsilon_0 + z\kappa , \quad (3)$$

where $\varepsilon$ is the axial strain of a point on the cross section with

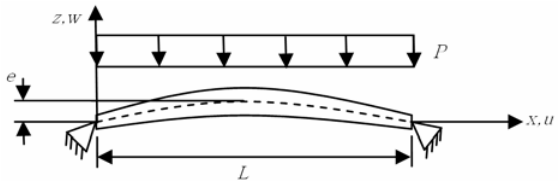


Fig. 1. Initial geometry of a shallow arch.

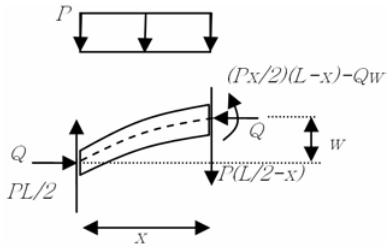


Fig. 2. Free body diagram of a section of the arch.

vertical coordinate z measured from the centerline. $\varepsilon_0$ and $\kappa$ are the axial strain of the centerline and the change in its curvature, respectively, which can be expressed by the following two relations:

$$\varepsilon_0 = u' + (w'^2 - w_0'^2)/2 , \quad (4)$$

$$\kappa = -(w'' - w_0'') . \quad (5)$$

In relation (4), $u$ is the axial displacement and the second term on the right is caused by the variation in arc length due to the deflection of the centerline [10]. The internal axial loading Q is constant throughout the centerline and is the result of the axial stress $\sigma=E\varepsilon$, i.e.,

$$Q = -\int_A \sigma dA = -EA(x)\varepsilon_0 \Rightarrow \frac{Q}{EA(x)} = -[u' + (w'^2 - w_0'^2)/2] , \quad (6)$$

where $A$ ($x$) is the variable area of the arch cross section. The displacements of the arch at the ends are zero; hence, integration of the above equation over the span of the arch and making use of symmetry yields

$$\frac{2Q}{E}\int_0^{L/2} \frac{dx}{A(x)} = -\int_0^{L/2} (w'^2 - w_0'^2)dx . \quad (7)$$

Eqs. (2) and (7) refer to the coupled governing equations used to find the lateral deflection $w$ and axial force $Q$ in the arch. Eq. (7) makes the set nonlinear and requires a numerical procedure for solving it. Fortunately, as seen in the next section, since $Q$ is constant, it is possible to solve Eq. (2) for deflection using an innovative method and substitution of the solution into (7), giving a relation for $Q$ to be used for obtaining the snap load. In this study, the cross section of the arch is considered to be rectangular and only its thickness (in $z$ direction) is varied. The depth (in $y$ direction) is considered to be constant and taken as unity. To parameterize these equations

and help with the non-dimensional investigation of the phenomenon, the following parameters are introduced:

$$\hat{x}=1+\frac{x}{L},\quad \hat{w}=\frac{w}{L},\quad R=\frac{e}{L},$$
$$B=\frac{PL^3}{2EI_1},\quad C=\frac{L}{\sqrt[3]{12I_1}},\quad D=\frac{QL^2}{EI_1} \tag{8}$$

where $I_1$ is the area moment of the inertia at the ends of the arch. The parametric axial coordinate $\hat{x}$ is introduced in such a way that it is used in the power-law representation of the variation of moment of inertia in the following form:

$$I(\hat{x})=I_1\hat{x}^n \qquad 1\le\hat{x}\le 1.5\,. \tag{9}$$

Its evaluation is meaningful for the end $x$=0. The limits in (9) correspond to one half of the arch span in order to maintain symmetry. From this, the variation of cross sectional area along the arch can be written as

$$A(\hat{x})=\sqrt[3]{12I_1}\,\hat{x}^{n/3} \qquad 1\le\hat{x}\le 1.5\,. \tag{10}$$

Therefore, the governing equations in the non-dimensional form can be written as

$$\ddot{\hat{w}}+\frac{D\hat{w}}{\hat{x}^n}=\frac{B(\hat{x}-1)(2-\hat{x})}{\hat{x}^n}-8R\,, \tag{11}$$

$$\frac{D}{6C^2}\int_1^{1.5}\frac{d\hat{x}}{\hat{x}^{n/3}}=-\int_1^{1.5}\dot{\hat{w}}^2d\hat{x}+\frac{8R^2}{3}\,, \tag{12}$$

where dot represents differentiation with respect to $\hat{x}$. Once the deflected curve is solved from (11), it can be substituted back into (12) and the relation between $D$ and $B$ (or $Q$ and $P$) can be obtained. The snap load is obtained as a limiting case (sometimes called the limit load) and just before the jump, the internal mechanical parameters of the arch, including $Q$, reach an extremum. Therefore, the equation from which the snap load can be obtained is

$$\frac{dB}{dD}=0\,. \tag{13}$$

This procedure is explained in the next section.

## 3. Analytical-numerical solution procedure

In this section, an innovative analytical procedure is proposed for solving Eq. (11). This equation is an ordinary differential equation with variable coefficients and its solution consists of homogeneous and particular parts, i.e.,

$$\hat{w}=\hat{w}_h+\hat{w}_p\,. \tag{14}$$

The homogeneous part satisfies the following governing equation as well as boundary conditions

$$\ddot{\hat{w}}_h+\frac{D\hat{w}_h}{\hat{x}^n}=0 \qquad \hat{w}_h(1)=\dot{\hat{w}}_h(1.5)=0\,. \tag{15}$$

This form satisfies the conditions of Sturm-Liouville theory (see [12] for example); hence, its solution can be expressed in terms of Bessel orthogonal functions (see [13] for example) as follows:

$$\hat{w}_h(x)=c_1\sqrt{\hat{x}}J_v(b\hat{x}^m)+c_2\sqrt{\hat{x}}Y_v(b\hat{x}^m)$$
$$v=-\frac{1}{n-2}\qquad m=-\frac{n}{2}+1\qquad b=\frac{2\sqrt{D}}{n-2} \tag{16}$$

where $J_v$ and $Y_v$ are the Bessel functions of order $v$ of the first and second kind, respectively, and $c_1$ and $c_2$ are the constants of integration.

Next, Lagrange's theorem [12], which states that if the homogenous solution of the second order ordinary differential equation $f(y'',y',x)=h(x)$, the equation can be written as $y_h=c_1y_1(x)+c_2y_2(x)$. The total solution of the ODE can be written as

$$y(x)=c_1y_1+c_2y_2-y_1\int\frac{y_2h(x)dx}{\omega(y_1,y_2)}+y_2\int\frac{y_1h(x)dx}{\omega(y_1,y_2)}\,,$$
$$\omega=\begin{vmatrix}y_1 & y_2\\ y_1' & y_2'\end{vmatrix} \tag{17}$$

where $\omega$ is the Wronskian of the solution of the homogenous part. Using this theorem, the total lateral deflection for the arch can be written as

$$\hat{w}(\hat{x})=c_1\sqrt{\hat{x}}J_v(b\hat{x}^m)+c_2\sqrt{\hat{x}}Y_v(b\hat{x}^m)$$
$$-\sqrt{\hat{x}}J_v(b\hat{x}^m)\int\sqrt{\hat{x}}Y_v(b\hat{x}^m)h(\hat{x})d\hat{x}\,, \tag{18}$$
$$+\sqrt{\hat{x}}Y_v(b\hat{x}^m)\int\sqrt{\hat{x}}J_v(b\hat{x}^m)h(\hat{x})d\hat{x}$$

where $h(\hat{x})$ is the right-hand side of Eq. (11) and the Wronskian turns out to be one. Using the following identities [13]

$$\int\hat{x}^kJ_v(b\hat{x}^m)d\hat{x}=\frac{2^{-(v+1)}b^v\hat{x}^{k_2}H}{mk_1\Gamma(v+1)}$$
$$\int\hat{x}^kY_v(b\hat{x}^m)d\hat{x}=\frac{1}{m}(2^{k_3}b^{-(1+k_3)}(\frac{-1}{k_2\pi}(2^{-mk_2}\hat{x}^{k_2}b^{mk_2}$$
$$\times H(\hat{x})\cos(\pi v)\Gamma(-v))-(2^{v-(1+k_3)}\hat{x}^{k_2-2vm}b^{v+(1+k_3)}$$
$$\times H(\hat{x})\Gamma(v))/(\pi(-v+k_1))\,, \tag{19}$$
$$k_1=\frac{v}{2}+\frac{k}{2m}+\frac{1}{2m}\qquad k_2=2mk_1$$
$$k_3=-1+\frac{k}{m}+\frac{1}{m}$$
$$H(\hat{x})=Hypergeom(k_1;k_2,1+k_1;-\frac{b^2\hat{x}^{2m}}{4})$$

where *Hypergeom* ( ) is the Hypergeometric function [12]. The lateral deflection $\hat{w}(\hat{x})$ is obtained analytically for every

value of the power-law exponent $n$ in terms of some known series functions. The final expression, however, is extremely long and is therefore not mentioned here.

Once the deflection is calculated, it is substituted into Eq. (12), a relation between $B$ and $D$ is obtained, and the relation (13) can be used to obtain the critical snap loading. Unfortunately, this part of the procedure cannot be performed analytically (the integration in (12) is quite complicated). Thus, the nonlinear equation resulting from (13) has to be solved using numerical techniques (this is a single variable highly nonlinear equation and to be solved efficiently, built-in solvers in mathematical software that work based on numerical optimization have to be utilized in this investigation).

Thus, for different values of the effective parameters and power-law exponent, this procedure can be performed and the value of the non-dimensional critical snap loading can be obtained. This is shown in the next section.

## 4. Numerical results and discussion

In this section, some results based on the procedure outlined in the previous section are presented. For the first case, the effect of power-law exponent on the critical snap-loading is investigated. This is carried out for a certain values of parameters introduced before. The set values are $R$=0.1 and $C$=$10^4$. Fig. 3 shows the result based on three methods: the Analytical-Numerical (AN) procedure given in Section 3; the Solving the Finite Difference (FD) form of Eqs. (11) and (12), changing values of external loading P and monitoring the deflection of a specific point along the arch, such as the middle point for the occurrence of the extremum (jumping condition); and the Finite Element (FE) modeling of the structure and increasing the external loading until a jump occurs. For the FD method, the number of discretization points along the $x$ axis is gradually increased until convergence occurs. For the FE method, commercial FEA software with suitable element type and meshing is utilized. There is good agreement between the three methods as shown in Fig. 3.

As expected, the critical loading increases as the power-law exponent increases. A couple of verifying data are also superimposed on the figure. Case $n$=0 corresponds to the constant thickness arch; the solution due to Timoshenko [1] is shown in the figure. Case $n$=2 also corresponds to an earlier work by Simitses [5], and its result is shown in the figure as well. There is good agreement between the previous results and those of the current research.

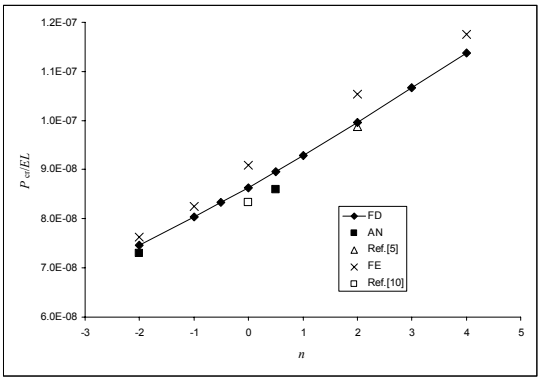


Fig. 3. Critical load for several power-law exponents using different methods.

To investigate the effect of variation in some parameters, some results are presented based on the AN method. Fig. 4 shows the effect of variation of parameter $R$ (shallowness of arch) on the critical loading for several power-law exponents. A value of $C$=$10^4$ is used. This parameter has a very significant effect in the increase of the critical loading.

The effect of parameter $C$ (slenderness of the arch) on critical loading is investigated. Fig. 5 shows the result for a typical value of power-law exponent (here $n$=2) for three values of $C$ equal to $10^3$, $5\times10^3$ , and $10^4$. The variation of $C$ causes the $I_1$ to change and, therefore, the non-dimensional ratio $P/EL$ is shown here. The value of $R$ is also varied. The effect of decrease of $C$ is more significant as R is increased. The summary of the effects of variation of $C$ and $R$ is shown as a 3D surface in Fig. 6.

An interesting case involving the effect of swapping the moment of inertia between the ends of the arch and the middle point, i.e., one arch narrowing and the other arch thickening toward the center, on the critical snap load at different values of the power-law exponent is investigated. Fig. 7 shows the result. Indices 1 and 2 correspond to the thickening and narrowing arches, respectively. For arch number 1, the moment of inertia increases from $I_1$ at the ends to $(1.5)^n I_1$ at the middle

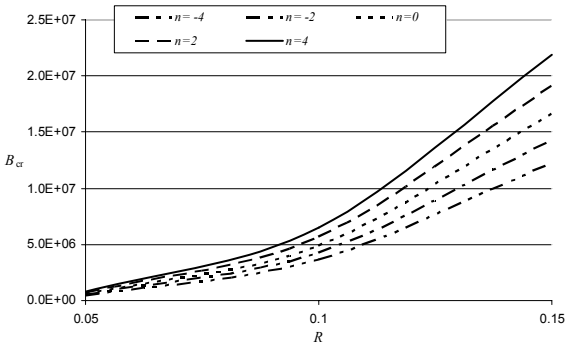


Fig. 4. Effect of $R$ on critical loading for several power-law exponents.

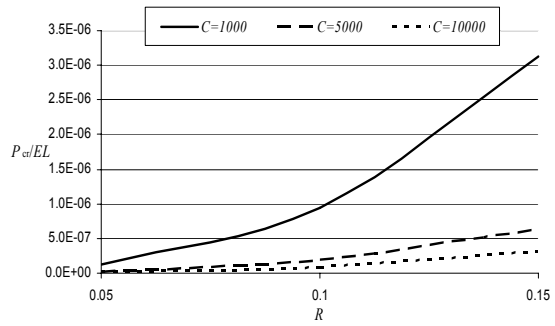


Fig. 5. Effect of $C$ on critical loading.

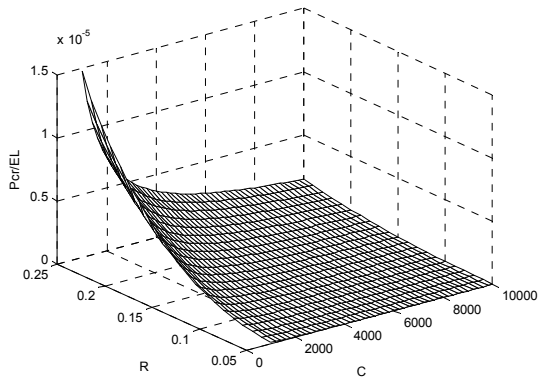


Fig. 6. 3D plot of parameter effects on critical loading ($n$=2).

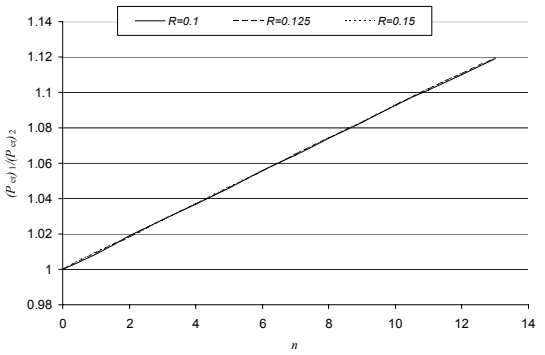


Fig. 7. Comparison of critical loading for thickening and narrowing arches.

point by the power-law $I = I_1\hat{x}^n$ . For arch number 2, the order is reversed by the power-law $I = 1.5^n I_1\hat{x}^{-n}$ . This is conducted for three different values of $R$. Arch 1 gives rise to a higher critical loading and the effect is the same irrespective of the value of $R$ and the ratio increases in an almost linear fashion with $n$. To justify this, note that the shape of the deformed centerline just before the jump is almost the same irrespective of the value of $I_1$ (within the range compatible with thin arch assumption) or the exponent $n$. This result makes the integral on the right side of Eq. (7) almost a constant; hence, the value of $Q$ depends only on the integral on the left. For negative values of $n$ in the case just mentioned, the left side integral is smaller compared to that of the corresponding positive n, making $Q$ smaller for negative $n$ (less axial pressure builds up before snap through) and lower snap loading.

For the last example, a case that can be of practical interest is considered. The aim in this case is to determine the effect varying thickness has on critical loading compared to a constant thickness arch with the same mass. Fig. 8 shows the outcome. The horizontal axis is the ratio of $I_1$ of the variable thickness to that of constant thickness arch (inertia ratios less than 1 correspond to positive values of the power law exponent). For this case, the shallowness parameter $R$ is taken to be 0.1. Surprisingly, constant thickness gives a higher critical load. This can be justified by noting that when the thickness varies, the integral on the left side of Eq. (7) is larger than that in the constant thickness case (this is the same as equivalent

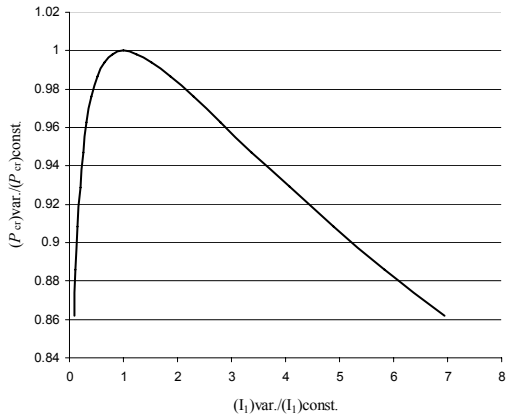


Fig. 8. Critical load for arches having the same mass.

stiffness for springs in series or equivalent resistance for resistors in parallel). Based on findings in the previous case, at the jump, the center line is almost similar in shape regardless of the way the thickness varies. Thus, the integral on the right remains almost the same. The resulting axial force $Q$ becomes smaller for the case of variable thickness, giving rise to a smaller critical load.

## 5. Conclusion

A mixed analytical-numerical method for obtaining snap load of power-law variable thickness shallow arch is presented. The agreement between the results from this method and those from other usual procedures is satisfactory. Based on these results, the decrease in slenderness ratio and shallowness parameter $C$ and the increase in shallowness parameter $R$ cause a higher critical loading. For arches having the same mass, variable thickness arches have lower critical loading compared to constant thickness arches.

## References

[1] S. P. Timoshenko, Buckling of Curved Bars with Small Curvature, *Journal of Applied Mechanics (ASME)*, 2 (1) (1935) 17.

[2] C. B. Biezeno, Das Durchschlagen eines schwach gekriimmten Stabes, Zeitschrift Angew. *Math, und Mech. (ZAMM)*, 18 (1938) 21-29.

[3] K. Marguerre, Die. Durchschlagskraft eines schwach gekrummten Balken, *Sitz. Berlin Math. Ges.*, 37 (92) (1938) 92-108.

[4] Y. C. Fung and A. Kaplan, Buckling of Low Arches of Curved Beams of Small Curvature, 1952, *NACA TN 2840.*

[5] G. J. Simitses and I. H. Rapp, Snapping of Low Arches with on-Uniform Stiffness, *Eng. Mech. (ASCE)*, 103 (1) (1977) 51-65.

[6] Y. L. Pi, M. A. Bradford and F. Tin-Loi, Nonlinear analysis and buckling of elastically supported circular shallow arches, *International Journal of Solids and Structures*, 44 (2007) 2401-2425.

[7] Y. L. Pi, M. A. Bradford and F. Tin-Loi, Non-linear in-plane buckling of rotationally restrained shallow arches under a central concentrated load, *International Journal of Non-Linear Mechanics*, 43 (2008) 1-17.

[8] C. A. Dimopoulos and C. J. Gantes, Nonlinear in-plane behavior of circular steel arches with hollow circular cross-section, *Journal of Constructional Steel Research*, 64 (2008) 1436-1445.

[9] Y. L. Pi and M. A. Bradford, Nonlinear in-plane elastic buckling of shallow circular arches under uniform radial and thermal loading, *International Journal of Mechanical Sciences*, 52 (1) (2010) 75-88.

[10] Z. P. Bazant and L. Cedolin, *Stability of Structures*, 2003, Dover Publications Inc.

[11] R. Eghtefari, *Analysis of snap-through in variable thickness arches*, M.Sc. Thesis, Islamic Azad University, Karaj Branch, Summer (2009) (in Persian).

[12] A. D. Polyanin and V. F. Zaitsev, *Handbook of Exact Solutions for Ordinary Differential Equations*, (2003) Chapman & Hall.

[13] B. G. Korenev, *Bessel functions and their applications*, 2002, Taylor & Francis.

**Ali Asghar Atai** received his B.Sc. in Mechanical Engineering from the University of Tehran, Iran, in 1990. He obtained his M.Sc. and Ph.D from the University of Alberta, Canada, in 1994 and 1998, respectively. He is currently a professor at the Department of Mechanical Engineering, Islamic Azad University, Karaj Branch, Iran. He is also a lecturer in the Department of Mechanical Engineering, University of Tehran. His areas of research interest include flexible structural mechanics, continuous media, and dynamics of machines.